Journal of Solid State Chemistry 181 (2008) 1848–1852

Contents lists available at ScienceDirect

Journal of Solid State Chemistry

journal homepage: www.elsevier.com/locate/jssc

Crystal structure and luminescence of $Sr_{0.99}Eu_{0.01}AlSiN_3$

Hiromu Watanabe [a,*], Hisanori Yamane [b], Naoto Kijima [a]

[a] Mitsubishi Chemical Group Science and Technology Research Center Incorporated, 1000 Aoba-ku, Yokohama, Kanagawa 227-8502, Japan
[b] Institute of Multidisciplinary Research for Advanced Materials, Tohoku University, 2-1-1 Katahira, Aoba-ku, Sendai 980-8577, Japan

ARTICLE INFO

Article history:
Received 10 March 2008
Accepted 17 April 2008
Available online 3 May 2008

Keywords:
High pressure N_2 gas synthesis
Nitride phosphor
Crystal structure
Single-crystal X-ray diffraction
Bond valence
Luminescence
Excitation and emission spectra

ABSTRACT

Strontium europium aluminum silicon nitride, $Sr_{0.99}Eu_{0.01}AlSiN_3$, was synthesized by heating a mixture of binary nitrides at 2173 K and a N_2 gas pressure of 190 MPa. Single crystals of $Sr_{0.99}Eu_{0.01}AlSiN_3$ approximately 30 μm were obtained. The structure was confirmed to be an isotypic structure of $CaAlSiN_3$ in the orthorhombic space group $Cmc2_1$, analyzed by single-crystal X-ray diffraction. The lattice parameters are $a = 9.843(3)$, $b = 5.7603(16)$, $c = 5.177(2)$ Å, cell volume = 293.53(17) Å^3. It shows an orange-red photoluminescence by $5d \rightarrow 4f$ transition of Eu^{2+} at around 610 nm under excitation ranging from ultraviolet to 525 nm. The photoluminescence intensity, temperature characteristics, and oxidative stability were comparable or superior to those of $CaAlSiN_3$:Eu^{2+} phosphor.

1. Introduction

Recently, a new class of red-emitting nitride phosphors has been studied and developed [1–3] for white LED use, which requires high luminescence efficiency under excitation at near-ultraviolet to blue light from InGaN diode. In paticular, $CaAlSiN_3$:Eu^{2+} is one of the most promising phosphors for practical application which requires saturated red, chemical stability, small thermal quenching, and high quantum efficiency [2,3]. X-ray powder diffraction patterns and lattice parameters of $CaAlSiN_3$ and $CaAlSiN_3$:Eu^{2+} have been reported in the previous studies [3–5]. Ottinger [6] analyzed the crystal structure of $CaAlSiN_3$ by single-crystal X-ray diffraction, and reported the orthorhombic cell parameters $a = 9.851(5)$, $b = 5.654(3)$, $c = 5.071(2)$ Å, cell volume = 282.2(2) Å^3, and space group $Cmc2_1$. The atomic and electronic structure of $CaAlSiN_3$ has also been studied by first-principles band calculations [7]. Decreasing the crystal field strength around Eu^{2+} will shift the emission peak position from deep red to orange. This has been shown previously by substitution of Ca^{2+} in $CaAlSiN_3$:Eu^{2+} partially by Sr^{2+} which has a larger ionic radius than Ca^{2+} [9]. $CaAlSiN_3$–$SrAlSiN_3$ solid solutions were investigated theoretically and experimentally by using polycrystalline samples [7,10]. In the present study, we performed the first complete substitution of Ca^{2+} with Sr^{2+} in $CaAlSiN_3$:Eu^{2+} by synthesis at high temperature and high N_2 gas pressure, analyzed the crystal structure by single-crystal X-ray diffraction, and characterized the photoluminescent properties.

2. Experimental

High-purity grade Si_3N_4 (Ube Industries, SN-E10, >99%), and AlN (Tokuyama, F-Grade, >99%) were used as received. $Sr_2N_{0.92}$ and $EuN_{1.0}$ were prepared by heating metals of Sr (Aldrich, 99%) and Eu (Aldrich, 99%) at 1123 K for 5 h under atmospheric pressure in purified N_2 (O_2, H_2O < 0.1 ppm), respectively. $Sr_2N_{0.92}$, $EuN_{1.0}AlN$, and Si_3N_4 were mixed in a Sr:Eu:Al:Si molar ratio of 0.992:0.008:1.00:1.00, and packed into a BN crucible in a N_2 gas-filled glove box. The BN crucible was loaded into a hot isostatic pressing apparatus equipped with a graphite heater (HIP). After several HIP evacuation/purge cycles with N_2, the N_2 pressure was raised to 50 MPa at room temperature, and then increased to 190 MPa by heating to 2173 K. After heating at 2173 K for 4 h, the product was cooled to 473 K, with a corresponding pressure of 70 MPa. The HIP apparatus was vented at this temperature followed by cooling to room temperature.

The as-prepared sample contained a mixture of colorless, amorphous compounds as major phases, and pale orange powder of $Sr_2Si_5N_8$:Eu^{2+} and $SrSiN_2$:Eu^{2+} and bright orange-red grains of $SrAlSiN_3$:Eu^{2+} as the minor phases. Since $SrAlSiN_3$:Eu^{2+} is stable against moisture and dilute acid, the crystals of $Sr_{0.99}Eu_{0.01}AlSiN_3$ were separated by repeated decantation and classification from the aqueous suspension. This was followed by removing the amorphous or unstable phases with dilute hydrochloric acid. After

* Corresponding author. Fax: +81 45 963 3652.
E-mail address: watanabe.hiromu@mh.m-kagaku.co.jp (H. Watanabe).

0022-4596/$ - see front matter © 2008 Elsevier Inc. All rights reserved.
doi:10.1016/j.jssc.2008.04.017

the separation, single crystals of $SrAlSiN_3$:Eu^{2+} were isolated by ultraviolet (UV)-blue lamp excitation and observing intense red photoluminescence (PL) under an optical microscope. A red transparent single crystal of $SrAlSiN_3$:Eu^{2+} with a size of $0.027 \times 0.027 \times 0.021\,mm^3$ was used for X-ray diffraction. The contents of Sr, Eu, Al, and Si in the single crystals were analyzed qualitatively with an energy dispersive X-ray (EDX) spectrometer (Horiba EMAX ENERGY) equipped with a scanning electron microscopy (SEM) (Hitachi S-3400N).

The X-ray diffraction data of the single crystal was collected with an imaging plate X-ray camera (Rigaku RAXIS-RAPID). Data reduction and cell refinement were carried out with the program PROCESS-AUTO [11]. Absorption was analytically corrected with the program NUMABS [12]. The initial model used for structure refinement was based on the atomic coordinates of $CaAlSiN_3$ reported by Ottinger [6]. The structure refinement was performed using SHELXL97 [13]. Softwares, ATOMS [14] and VESTA [15] were used for drawing the structure.

PL spectra at room temperature were measured by an optical multichannel analyzer (Hamamatsu Photonics C7041) equipped with a Xe lamp. The wavelength resolution was 1 nm. Excitation spectra were measured by a spectrofluorometer (Hitachi F-4500). Temperature dependence of PL was measured with an apparatus (Otsuka Electronics MCPD7000) equipped with temperature controlling sample holders and a Xe lamp.

3. Results and discussion

The chemical composition was determined to be $Sr_{0.99}Eu_{0.01}AlSiN_3$ (Sr:Eu:Al:Si = 0.99:0.01:1:1.02) by EDX analysis. The crystal data and structure refinement are shown in Table 1. The refinement of the Flack parameter [16,17] was obtained by way of TWIN/BASF instructions of SHELXL97 [13]. The Flack parameter indicates a 0.43(4):0.57 ratio of two possible polarities of the structure. The atomic positions and anisotropic displacement parameters are listed in Tables 2 and 3. One of the three principal mean square atomic displacements for the N1 site tended to a small positive or negative value when the refinement included anisotropic displacement parameters. Thus, all N-atom sites were refined with isotropic displacement parameters.

Table 1
Structure refinement and crystallographic data for $Sr_{0.99}Eu_{0.01}AlSiN_3$

Empirical formula	$Sr_{0.99}Eu_{0.01}AlSiN_3$
Formula weight	185.36
Temperature	293(2) K
Diffractometer type	Rigaku RAXIS-RAPID
Scan mode	ω
Crystal system	Orthorhombic
Space group	$Cmc2_1$ (no. 36)
Unit cell dimensions	
a (Å)	9.843(3)
b (Å)	5.7603(16)
c (Å)	5.177(2)
Volume (Å^3)	293.53(17)
Calculated density (g cm^{-3})	4.195
Z	4
Wavelength	0.710747 Å (Mo $K\alpha$)
Absorption coefficient	18.833 mm^{-1}
Crystal shape, color	Granule, red
Crystal size	$0.027 \times 0.027 \times 0.021\,mm^3$
Absorption correction	Numerical (NUMABS; Higashi, 1999)
Max. and min. transmission	0.721 and 0.772
Reflection collected	1353
Independent reflections	355 ($R_{int} = 0.050$), (338 $I > 2\sigma(I)$)
θ Range for data collection	4.10–27.44°
Limiting indices	$h = -12 > 12$, $k = -7 > 6$, $l = -6 > 6$
Refinement method	Full-matrix least squares on F^2
Final R indices	$R\,[F^2 > 2\sigma(F^2)] = 0.0325$, $wR(F^2) = 0.0814$
Goodness-of-fit on F^2	1.068
Data/restraints/ parameters	355/0/25
Extinction coefficient	0.014(2)
Flack parameter	0.43(4)
Weight	$w = 1/[\sigma^2(F_o^2)+(0.0452P)^2+2.2659P]$, where $P = (F_o^2+2F_c^2)/3$
Largest diff. peak and hole	0.778 and −0.865 e Å^{-3}

Table 2
The atomic coordinates, occupancies, and isotropic atomic displacement parameters of $Sr_{0.99}Eu_{0.01}AlSiN_3$

Atom	Site	Occ.	x	y	z	U_{eq}(Å^2)[a]
$Sr_{0.99}Eu_{0.01}AlSiN_3$						
Al/Si	8*b*	0.50/0.50	0.1777(2)	0.1518(4)	0.0256(17)	0.0141(7)
N1	8*b*	1.00	0.2286(8)	0.1177(14)	0.3617(14)	0.0217(17)
N2	4*a*	1.00	0	0.2081(13)	0.015(6)	0.0189(19)
Sr/Eu	4*a*	0.99/0.01	0	0.31526(13)	0.5086	0.0105(4)

[a] U_{eq} is defined as one-third of the trace of the orthogonalized U_{ij} tensor.

Table 3
Anisotropic displacement parameters (Å$^2 \times 10^3$) for $Sr_{0.99}Eu_{0.01}AlSiN_3$

	U_{11}	U_{22}	U_{33}	U_{23}	U_{13}	U_{12}
Al/Si	0.0142(9)	0.0164(10)	0.0116(17)	0.0013(18)	−0.0002(17)	0.0007(7)
Sr/Eu	0.0112(5)	0.0126(5)	0.0078(5)	−0.0001(7)	0	0

The anisotropic displacement factor exponent takes the form: $-2\pi^2[h^2a^{*2}U_{11}+\cdots+2hka^*b^*U_{12}]$.

$Sr_{0.99}Eu_{0.01}AlSiN_3$ is isostructural with $CaAlSiN_3$, $NaSi_2N_3$, $LiSi_2N_3$, and $NaGe_2N_3$ [2,6–8,18]. As described in the previous reports [3,6–8], the structure of $CaAlSiN_3$ is related to the hexagonal wurtzite-type structure with space group, $P6_3mc$, which is a minimal non-isomorphic supergroup of $Cmc2_1$. The cell volume increased 4% by the substitution of Sr for Ca. The *b*- and *c*-axis lengths of $Sr_{0.99}Eu_{0.01}AlSiN_3$ are approximately 2% larger than those of $CaAlSiN_3$, but the *a*-axis length is 0.1% smaller. The ratios $a/b = 1.709$ and $c/(b/\sqrt{3}) = 1.557$ for $Sr_{0.99}Eu_{0.01}AlSiN_3$ indicate that the structure is fairly distorted from the ideal wurtzite-type structure ($a/b = \sqrt{3} = 1.732$, $c_H/a_H = \sqrt{8}/3 = 1.633$). Although the theoretically calculated cell parameters of $SrAlSiN_3$ ($a = 9.9201$, $b = 5.7792$, and $c = 5.2003$ Å) are, 0.3–0.8% larger than the parameters of the present study [8], the calculated values are within the typical theoretical errors of 1–2%. The ratios of the theoretical parameters $a/b = 1.7165$ and $c/(b/\sqrt{3}) = 1.5585$ are similar to those observed for $Sr_{0.99}Eu_{0.01}AlSiN_3$.

The crystal structure of $Sr_{0.99}Eu_{0.01}AlSiN_3$ is shown in Fig. 1. Selected interatomic distances and bond angles are listed in Table 4. Al and Si atoms that statistically occupy an 8*b* site [7] are tetrahedrally coordinated by three N1 and one N2 atoms. The average Al/Si–N interatomic distances and the tetrahedron distortion index [19] are 1.816 Å and 0.010, respectively. The average interatomic distance is close to the average of typical bond length of Si–N and Al–N [7]. The bond valence sum (BVS) [20,21] of 3.54 calculated for the Al/Si site with the bond valence parameter $B_{0(Si-N)} = 1.77$ Å was consistent with the formal charge +3.5 of $0.5Si^{4+}$+$0.5Al^{3+}$. N1 atom is in the triangular plane of the Al/Si atoms with bond distances of 1.821(11)−1.839(9) Å and Al/Si–N1–A/Si angles of 117.2(3)−122.5(7)°. Two Al/Si atoms bond to an N2 atom with a bond length of 1.780(3) Å and Al/Si–N1–Al/Si^i angle of 158.7(7)°.

All Al/Si–N_4 tetrahedra are connected to each other by sharing all N atoms, forming a network structure with six-membered

rings in the *a*–*b* plane, as illustrated in Fig. 2. Sr and Eu atoms are situated in the cage of the tetrahedra network. It has been described that Ca atoms in $CaAlSiN_3$ are coordinated by five atoms with a BVS of 1.928 [3,7]. The interatomic distances between five first nearest nitrogen atoms and the Sr/Eu atom are 2.63(3)–2.746(8) Å. However, the BVS of the five Sr–N bond valences calculated with the parameter $B_{0(Sr-N)} = 2.23$ Å [21] is 1.56, which is far from the expected valence of 2.0. When bond valences to the second nearest nitrogen atoms with interatomic distances from 3.015(8) to 3.279(8) Å are added, the BVS is 1.90. In this case, the Sr/Eu site is surrounded by 10 nitrogen atoms.

By taking into account the Sr/Eu–N distances within 3.279(8) Å, the N1 atom is surrounded by three Al/Si atoms and three Sr/Eu atoms as shown in Fig. 1. The N2 atom is in the octahedron of two Al/Si and four Sr/Eu atoms. The N1 and N2 atoms are in six-fold environments and the BVSs calculated with the bond valence parameters of Si–N and Sr–N are 3.02 for N1 and 2.94 for N2. These BVS values coincide with the formal valence III (or formal charge −3) of nitrogen. Fig. 3 shows the crystal structure of

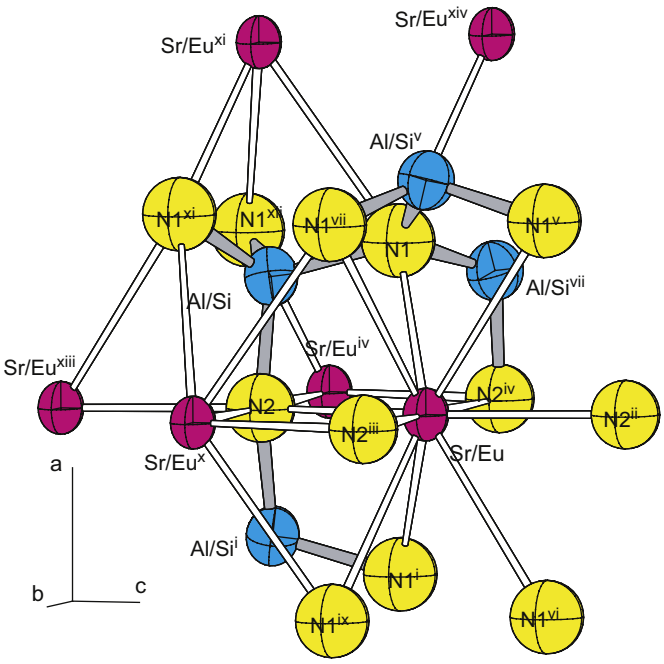

Fig. 1. The crystal structure of $Sr_{0.99}Eu_{0.01}AlSiN_3$. Displacement ellipsoids are drawn at the 99% probability level. Symmetry codes represented in Table 4.

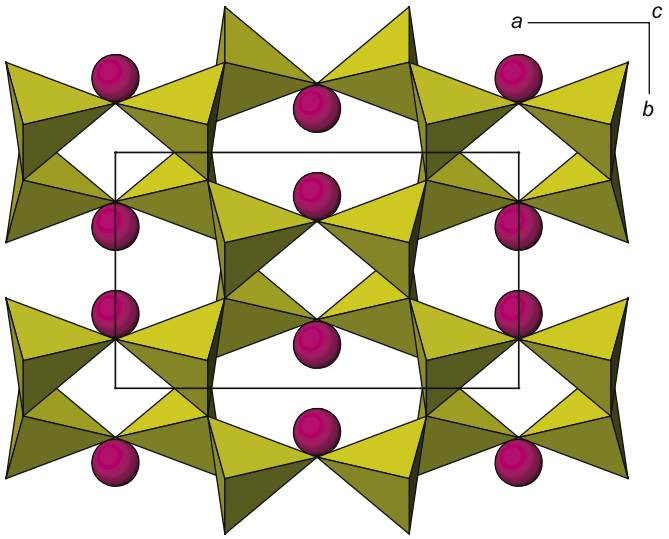

Fig. 2. Projective representation of the crystal structure of $Sr_{0.99}Eu_{0.01}AlSiN_3$ illustrated with Al/Si-centered nitrogen tetrahedra.

Table 4
Selected geometric parameters (Å, deg.) of $Sr_{0.99}Eu_{0.01}AlSiN_3$

	Distance	BV(Sr–N)[a]		Distance	BV(Sr–N)[a]
Sr/Eu–N2	2.63(3)	0.342	N1–Al/Si	1.821(12)	0.870
Sr/Eu–N1^{i}	2.634(8)	0.336	N1–Al/Si^{v}	1.825(9)	0.861
Sr/Eu–N1	2.634(8)	0.336	N1–Al/Si^{vi}	1.839(10)	0.831
Sr/Eu–N2^{ii}	2.70(3)	0.284	N1–Sr/Eu	2.634(8)	0.336
Sr/Eu–N2^{iii}	2.746(8)	0.248	N1–Sr/Eu^{xi}	3.260(8)	0.062
Sr/Eu–N2^{iv}	3.015(8)	0.120	N1–Sr/Eu^{xiv}	3.279(8)	0.059
Sr/Eu–Al/Si^{v}	3.179(2)		BVS (Si–N,–Sr)[a]		3.019
Sr/Eu–Al/Si^{vi}	3.179(2)				
Sr/Eu–Al/Si^{i}	3.194(7)		N2–Al/Si	1.780(3)	0.973
Sr/Eu–Al/Si	3.194(7)		N2–Al/Si^{i}	1.780(3)	0.973
Sr/Eu–Al/Si^{iv}	3.211(2)		N2–Sr/Eu	2.63(3)	0.342
Sr/Eu–Al/Si^{vii}	3.211(2)		N2–Sr/Eu^{xiii}	2.70(3)	0.284
Sr/Eu–N1^{v}	3.260(8)	0.062	N2–Sr/Eu^{x}	2.746(8)	0.248
Sr/Eu–N1^{vi}	3.260(8)	0.062	N2–Sr/Eu^{iv}	3.015(8)	0.120
Sr/Eu–N1^{viii}	3.279(8)	0.059	BVS (Si–N,–Sr)[a]		2.940
Sr/Eu–N1^{ix}	3.279(8)	0.059			
BVS (Sr–N)[a]		1.898	Al/Si–Al/Si^{viii}	3.213(3)	
			Al/Si–Al/Si^{i}	3.498(3)	

	Distance	BV(Sr–N)[a]		Angle
Al/Si–N2	1.780(3)	0.973	Al/Si^{v}–N1–Al/Si	120.3(3)
Al/Si–N1	1.821(12)	0.870	Al/Si^{v}–N1–Al/Si^{vii}	122.5(3)
Al/Si–N1^{xiv}	1.825(9)	0.861	Al/Si–N1–Al/Si^{vii}	117.2(3)
Al/Si–N1^{xv}	1.839(10)	0.831	Al/Si–N2–Al/Si^{i}	158.7(7)
Average	1.816		Al/Si–Al/Si^{viii}–Al/Si^{xv}	127.41(7)
BVS (Si–N)[a]		3.535		

Symmetry codes: (i) $-x, y, z$; (ii) $x, y, z+1$; (iii) $-x, -y+1, z+1/2$; (iv) $-x, -y, z+1/2$; (v) $-x+1/2, -y+1/2, z+1/2$; (vi) $x-1/2, -y+1/2, z+1/2$; (vii) $x, -y, z+1/2$; (viii) $-x+1/2, y+1/2, z$; (ix) $x-1/2, y+1/2, z$; (x) $-x, -y+1, z-1/2$; (xi) $-x+1/2, -y+1/2, z-1/2$; (xii) $x, -y, z-1/2$; (xiii) $x, y, z-1$; (xiv) $x+1/2, y-1/2, z$; (xv) $x, 1+y, z$.

[a] Bond valence (BV) and bond valence sum (BVS) [21,22].

$Sr_{0.99}Eu_{0.01}AlSiN_3$ illustrated with the N2 atom-centered Sr/Eu–Al/Si octahedra which share Sr/Eu–Sr/Eu edges and form layers in the b–c plane at $x = 0.0$ and 0.5.

Fig. 4 compares the crystal structures of $CaAlSiN_3$ and $Sr_{0.99}Eu_{0.01}AlSiN_3$ projected on the a–b plane. The average Al/Si–N interatomic distances and tetrahedron distortion indexes of $CaAlSiN_3$ (1.814 Å and 0.007) are close to those of $Sr_{0.99}Eu_{0.01}AlSiN_3$ (1.816 Å and 0.010). However, angles of Al/Si–N2–Al/Si^{i} and Al/Si–Al/Si^{viii}–Al/Si^{xv} of $Sr_{0.99}Eu_{0.01}AlSiN_3$ in the a–b plane are larger than those of $CaAlSiN_3$, which correspond to a thicker octahedral layer and a smaller distance between the octahedral layers. The octahedral layer thickness indicated with Al/Si–Al/Si^{i} (3.498(3) Å) is 1.7% larger than that of $CaAlSiN_3$, which indicates a nearly isotropic volume increase for the N2-centered octahedral layer by Sr/Eu substitution. The decrease of the interlayer distance relates to the tilting of the N1-centered triangular $(Al/Si)_3$, resulting in the slight decrease of the a-axis length.

The excitation and emission spectra of $Sr_{0.99}Eu_{0.01}AlSiN_3$ at room temperature are shown in Fig. 5. A broad absorption band extended over the UV region to approximately 500 nm. The emission peak of $5d \rightarrow 4f$ transition of Eu^{2+} was centered around 610 nm by excitation of blue light (455 nm). The peak intensity was 20% greater, and the full-width at half-maximum was 20% narrower than those measured at 650 nm under the same instrumental condition for $CaAlSiN_3$:Eu^{2+} phosphor [2]. The 40 nm blue shifted emission peak results from weakening in the crystal field around Eu^{2+} compared to that of $CaAlSiN_3$:Eu^{2+}. The average distances from Ca and Sr/Eu to the five nearest N atoms are 2.498 [6] and 2.667 Å, respectively.

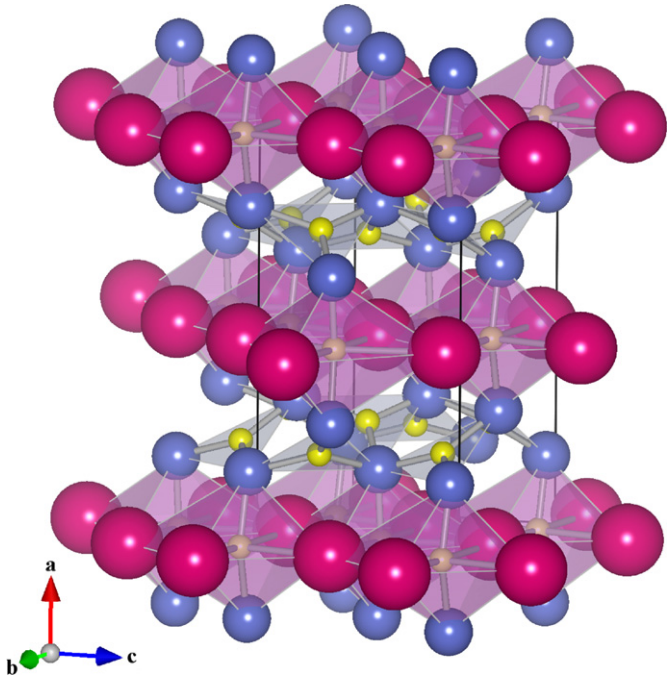

Fig. 3. The crystal structure representation of $Sr_{0.99}Eu_{0.01}AlSiN_3$ in a N2-centered Sr/Eu–Al/Si octahedra.

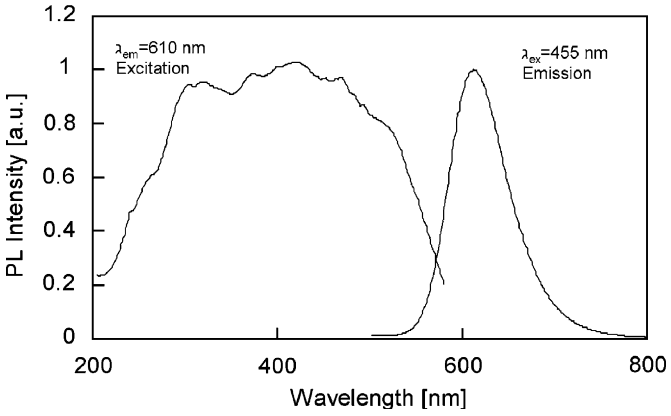

Fig. 5. Excitation and emission spectra of $Sr_{0.99}Eu_{0.01}AlSiN_3$.

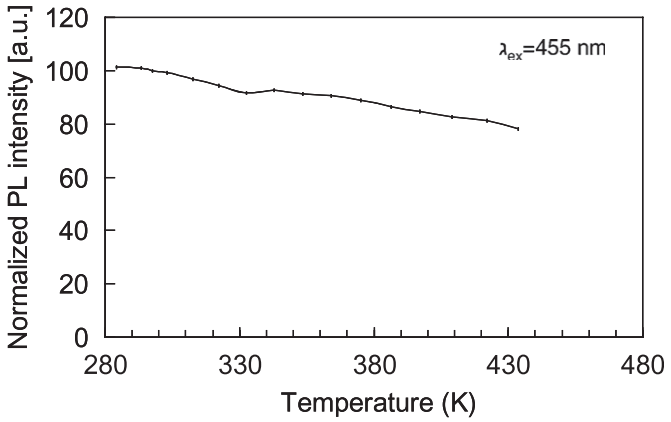

Fig. 6. Temperature dependence of emission intensity measured for $Sr_{0.99}Eu_{0.01}AlSiN_3$ at 610 nm × 455 nm excitation.

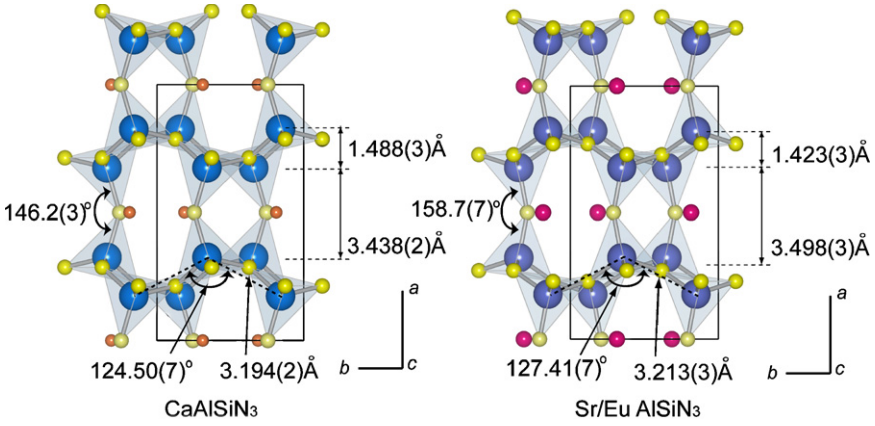

Fig. 4. Comparison of the crystal structures of $CaAlSiN_3$ and $Sr_{0.99}Eu_{0.01}AlSiN_3$ projected on the a–b plane.

The emission intensity of $Sr_{0.99}Eu_{0.01}AlSiN_3$ decreased slightly with increasing temperature, stabilizing at 80% of the intensity at 430 K from that of room temperature as shown in Fig. 6. This small thermal quenching character is also comparable with that of $CaAlSiN_3$:Eu^{2+}. Furthermore, no irreversible degradation of the emission from $Sr_{0.99}Eu_{0.01}AlSiN_3$ was detected after heating to 673 K for several hours in air, indicating the high resistance against oxidation.

4. Conclusions

Single crystals of $Sr_{0.99}Eu_{0.01}AlSiN_3$ were prepared by heating at 2173 K under a high pressure, 190 MPa, N_2 gas. The X-ray single-crystal diffraction data revealed that the structure is isotypic with that of $CaAlSiN_3$. While the *b*- and *c*-axis lengths and cell volumes of $Sr_{0.99}Eu_{0.01}AlSiN_3$ are larger than that of $CaAlSiN_3$, the *a*-axis length is slightly shorter. The crystal structures could be represented with a layer of the edge-sharing nitrogen-centered $(Sr/Eu)_4$–$(Al/Si)_2$ octahedra perpendicular to the *a*-axis, as well as with the conventional network of corner-nitrogen sharing tetrahedra. The volume of the octahedra containing Sr^{2+}/Eu^{2+} expanded almost isotropically, but the interlayer distance decreased by the substitution of Sr/Eu for Ca. The emission peak from Eu^{2+} in $Sr_{0.99}Eu_{0.01}AlSiN_3$ was observed at 610 nm by excitation with 455 nm light.

Acknowledgments

The authors wish to thank to Dr. Masayoshi Mikami, Dr. Kyota Uheda, and Dr. Hiroyuki Imura for frequent, stimulating and helpful discussions. The authors also wish to thank to Dr. Jeffrey Gerbec for his advice and careful reading of the manuscript.

Appendix A. Supplementry material

Further details of the crystal structure investigation can be obtained from the Fachinformationszentrum Karlsruche, 76344 Eggenstein-Leopoldshafen, Germany, (fax: (49)7247-808-666; e-mail: crysdata@fiz-karlsruhe.de) on quoting the depositry number CSD419410.

References

[1] Y.Q. Li, J.E.J. van Steen, J.W.H. van Krevel, G. Botty, A.C.A. Delsing, F.J. DiSalvo, G. de With, H.T. Hintzen, J. Alloys Compd. 417 (2006) 273.
[2] K. Uheda, N. Hirosaki, Y. Yamamoto, A. Naito, T. Nakajima, H. Yamamoto, Electrochem. Solid-State Lett. 9 (2006) H22.
[3] K. Uheda, N. Hirosaki, H. Yamamoto, Phys. Status Solidi A 203 (2006) 2712.
[4] J. Li, T. Watanabe, H. Wada, T. Setoyama, M. Yoshimura, Chem. Mater. 19 (2007) 3592.
[5] X. Piao, K. Machida, T. Horikawa, H. Hanzawa, Y. Shimomura, N. Kijima, Chem. Mater. 19 (2007) 4592.
[6] F. Ottinger, Ph.D. Thesis, Diss. ETH Nr. 15624 (2004).
[7] M. Mikami, K. Uheda, N. Kijima, Phys. Status Solidi A 203 (2006) 2705.
[8] M. Mikami, H. Watanabe, K. Uheda, N. Kijima, Mater. Res. Soc. Symp. Proc. 1040E (2008) 1040–Q10–09.
[9] R.D. Shannon, Acta Crystallogr. A 32 (1976) 752.
[10] H. Watanabe, H. Wada, K. Seki, M. Itou, N. Kijima, J. Electrochem. Soc. 155 (2008) F31.
[11] PROCESS-AUTO. Rigaku/MSC, 9009 New Trails Drive, The Woodlands, TX 77381-5209, USA.
[12] T. Higashi, NUMABS, Rigaku Corporation, Tokyo, Japan, 1999.
[13] G.M. Sheldrick, SHELXL97, University of Göhottingen, Göhottingen, Germany, 1997.
[14] E. Dowty, ATOMS, ver. 6.2. Shape Software, Kingsport, TN, USA.
[15] K. Momma, F. Izumi, Commission on Crystallogr. Comput., IUCr Newslett. 7 (2006) 106.
[16] H.D. Flack, Acta Crystallogr. A 39 (1983) 876.
[17] H.D. Flack, G. Bernardinelli, J. Appl. Cryst. 33 (2000) 1143.
[18] H. Jacobs, H. Mengis, Eur. J. Solid State Inorg. Chem. 30 (1993) 45.
[19] W.H. Baur, Acta Crystallogr. B 30 (1974) 1195.
[20] I.D. Brown, D. Altermatt, Acta Crystallogr. B 41 (1985) 244.
[21] N.E. Brese, M. O'Keeffe, Acta Crystallogr. B 47 (1991) 192.